Eur Biophys J (2004) 33: 412–420
DOI 10.1007/s00249-003-0375-y

ARTICLE

Mihaela Gheorghiu · Willy Van Driessche

Modeling of basolateral ATP release induced by hypotonic treatment in A6 cells

Received: 6 August 2003 / Revised: 30 October 2003 / Accepted: 11 November 2003 / Published online: 9 January 2004

Abstract ATP is released from the basolateral membrane of A6 epithelia in response to hypotonic treatment. This study addresses the problem of ATP diffusion through the permeable supports used to culture the cells. A theoretical analysis of a recently introduced experimental protocol is presented and a model of ATP diffusion through the compartments of the measuring system is proposed. The model provides the ATP profiles near the cell layer and in the measurement chamber. Comparison of results from computer simulations and experimental data showed that the permeable support introduces a marked delay for ATP diffusion, supporting the correlation of apparently time-separated events: the mobilization of Ca^{2+} from internal stores and release of ATP from the cell. The model is consistent with experimental data obtained with the luciferin–luciferase pulse protocol and provides an indirect proof of related processes like the closure and opening of the lateral interspace that occur after imposing the hyposmotic shock. The influence of the pore structure of the permeable support in modulating the measured release rates revealed by computer simulation is experimentally validated for two types of Anopore filters.

Keywords Epithelia · Diffusion model · Osmotic shock · Luminescence

M. Gheorghiu (✉)
International Centre of Biodynamics,
Calea Plevnei 46–48,
010233 Bucharest 1, Romania
E-mail: mgheorghiu@biodyn.ro
Tel.: +40-21-3104354
Fax: +40-21-3104361

W. Van Driessche
Laboratory of Physiology, K.U. Leuven,
Campus Gasthuisberg O/N,
3000 Leuven, Belgium

Introduction

In addition to its ubiquitous function as a main intracellular energy source, there is increasing evidence that, in non-excitable tissues, extracellular ATP plays an important role in auto- and paracrine feedback regulation of a broad range of cellular responses (Burnstock 1997). Release of ATP has been demonstrated in response to osmotic and mechanical stress (Grygorczyk and Hanrahan 1997; Taylor et al. 1998; Van der Wijk et al. 1999; Kimura et al. 2000; Mitchell 2001; Romanello et al. 2001) and neuro-hormonal stimuli, shedding some light over the possible release mechanisms, whereas the identification of the involved pathways is still uncertain. Several hypotheses concerning the pathways of ATP release have been proposed in recent years [ranging from a conductive pathway to a vesicular release mechanism (Knight et al. 2002)]. Connexin hemichannels have been identified as a signaling pathway that couples ATP liberation to intracellular Ca^{2+} changes after mechanical stimulation of astrocytes (Stout et al. 2002), but involvement of the cystic fibrosis transmembrane conductance regulator (CFTR) (Braunstein et al. 2001), of the related multidrugresistance-1 protein (Roman et al. 2001) and large conductance anion channels (Bell et al. 2003) in regulating the membrane permeability for ATP are still controversial.

The uncertainties concerning the identity of pathways underlying ATP release partially stem from a variety of methodological problems in assaying ATP release. The most commonly and sensitive technique used for detection of ATP release is based on the luminescence that follows oxidation of luciferin upon catalysis by luciferase in the presence of oxygen, Mg^{2+} and ATP. When using this principle to determine the ATP released from the basolateral membrane of polarized epithelia, the assay is confounded by a multitude of factors, including: (1) ATP release by mere mechanical stimulation, (2) effects of unstirred layers, (3) sequestration of ATP released into the microdomains of the lateral intercellular

spaces (LIS), (4) lack of selective inhibitors that modulate ATP release through candidate ion channels, (5) extremely low levels of release coupled with rapid extracellular ATP hydrolysis by membrane-bound ecto-ATPases, (6) consumption of ATP by the assay reaction itself, and last but not the least (7) the diffusional barrier represented by the permeable support over which cells were grown to confluent layers.

Recent experiments demonstrated that a sudden hyposmotic shock gives rise to a biphasic $[Ca^{2+}]_i$ upturn (Jans et al. 2002). The first rapid phase is inhibited by the presence of basolateral suramin, a purinergic (P2) receptor antagonist, indicating an autocrine effect induced by ATP. The relation between ATP release and $[Ca^{2+}]_i$ rise has been further explored (Jans et al. 2002), but a direct correlation between ATP release and the suramin-sensitive increase in $[Ca^{2+}]_i$ during hypotonicity was shadowed by the time lag between the $[Ca^{2+}]_i$ peak occurring at 45 s after the initiation of the hyposmotic shock and the maximum in measured ATP amounts appearing 6 min after the initiation of osmotic shock.

As a first step in elucidating the causal link between ATP release and the mobilization of Ca^{2+} from intracellular stores, the problem of ATP diffusion through the permeable support, acting as a diffusion barrier and delaying the ATP recordings, has to be analysed. The aim of this study is to address, from both experimental and theoretical points of view, the influence of the permeable filter support on the diffusion of ATP into the measurement chamber and to provide an insight into the possible dynamics of the ATP release through the basolateral membrane in relation to the characteristic pattern of ATP accumulation in the measurement chamber.

Materials and methods

Cell culture

The amphibian A6 renal cell line (a gift of Dr J.P. Johnson, University of Pittsburgh, Pittsburgh, Pa., USA) is derived from the distal part of the nephron of *Xenopus laevis*. A6 cells were grown on two types of permeable Anopore filters (Nunc Intermed, Roskilde, Denmark) in a humidified incubator maintained at 28 °C and 1% CO_2. We used 60 μm thick filters, 25.4 mm diameter, with pore sizes of 0.2 μm (relative porosity 30%) and 0.02 μm (relative porosity 50%). Cells were seeded at a density of 2×10^5 cm^{-2}. The growth medium was renewed twice weekly and consisted of a 1:1 mixture of Leibovitz's L-15 and Ham's F-12 media, supplemented with 10% fetal bovine serum (Sigma, St. Louis, Mo., USA), 3.8 mM L-glutamine, 2.6 mM $NaHCO_3$, 95 IU mL^{-1} penicillin and 95 mg mL^{-1} streptomycin. We used confluent, polarized monolayers cultured for 8–9 days. The tightness of the monolayer was tested by recording the transepithelial resistance.

Solutions and chemicals

Hyposmotic solutions of 140 mosmol $(kg\ H_2O)^{-1}$ contain (in mM): 70 Na^+, 2.5 K^+, 1 Ca^{2+}, 5 Hepes and 69.5 Cl^- (pH 7.4). Isosmotic solutions of 260 mosmol $(kg\ H_2O)^{-1}$ were prepared by adding 65 mM NaCl. The amount of ATP release in the basolateral compartment was determined with a luciferin–luciferase kit from Sigma (FL-AAM). The solutions that we used to probe for ATP release contained 50 μL of the luciferin–luciferase (LL) assay mixture per mL. This resulted in a final concentration for the following components (in mM): 0.5 $MgSO_4$, 0.05 EDTA, 0.005 dithiothreitol, 2.5 tricine and 0.03 luciferin; and (in mg L^{-1}): 3.3 luciferase and 50 bovine serum albumin.

Measurement of ATP release

We used a custom-designed setup that enables the quantification of the extracellular ATP amount in the measurement chamber via photo-detection of the light emitted during luciferase-catalysed oxidative decarboxylation of luciferin (LH_2), in the presence of ATP, Mg^{2+} and O_2 (Gomi and Kajiyama 2001):

$$\begin{aligned} &LH_2 + ATP \xrightarrow[\text{luciferase}]{Mg^2} \text{luciferase} \bullet LH_2 - AMP + PPi \\ &\text{luciferase} \bullet LH_2 - AMP + O_2 \rightarrow \text{luciferase} + AMP \\ &\quad + CO_2 + \text{oxyluciferin} + h\nu \end{aligned} \tag{1}$$

The setup is shown schematically in Fig. 1A. It uses a photon-counting head with a broad dynamic range, enabling the detection of amounts of ATP extending from 0.1 pmol to 25 nmol with 50 μL mL^{-1} LL reagent mixture. An important advantage of this setup is the availability of continuous perfusion of the polarized monolayer, allowing a fast replacement of solutions at each border. Moreover, removal of the permeable support from the culture cup is unnecessary, thus avoiding cell damage at the edges. The experimental set-up is described in detail elsewhere (Jans et al. 2002).

The measurement can be carried out either through a pulse protocol or by continuously recording the light originating from ATP accumulation in the basolateral compartment (the measurement chamber) containing the LL reagent that is well mixed. The pulse protocol consists of repeated periods of wash-out of the ATP and LL additions alternated by 90-s intervals when ATP accumulation was monitored. At the beginning of these intervals, the solution containing the LL reagent is injected into the measurement chamber. The pulse protocol implies that the accumulation of released ATP is measured at defined moments, with the initial ATP amount in the bath reset to zero by continuous perfusion of hyposmotic solution. The LL assay kit is refreshed for each pulse. The initial rate of rise of the luminescence, proportional to the ATP release, is determined by regression analysis. For clarity, the term "released" will be used for the ATP leaving the filter while "generated" will be used for the ATP leaving the basolateral membrane, at the upper side of the filter.

In the accumulation protocol the LL assay mixture is added to the basolateral chamber and the perfusion is suspended to allow the accumulation of ATP. The continuous recordings provide a time evolution dependent on both the release rate and the consumption/dissociation coefficients of the experiment. The accumulation protocol implies that the amassment of released ATP is assessed in the measurement chamber in which a certain amount of LL kit is injected at the beginning of the recording and not replenished in the meantime.

Computer simulations and modeling

The process of diffusion, through which matter is transported from one part of a system to another as a result of random molecular motion, becomes particularly important when trying to establish causal links between spatially separated events by creating new "dynamics". Owing to a slower effective diffusion, the rapid changes in one compartment might be translated into slowly changing concentrations in another compartment, dampening the "fluctuations" or transient changes.

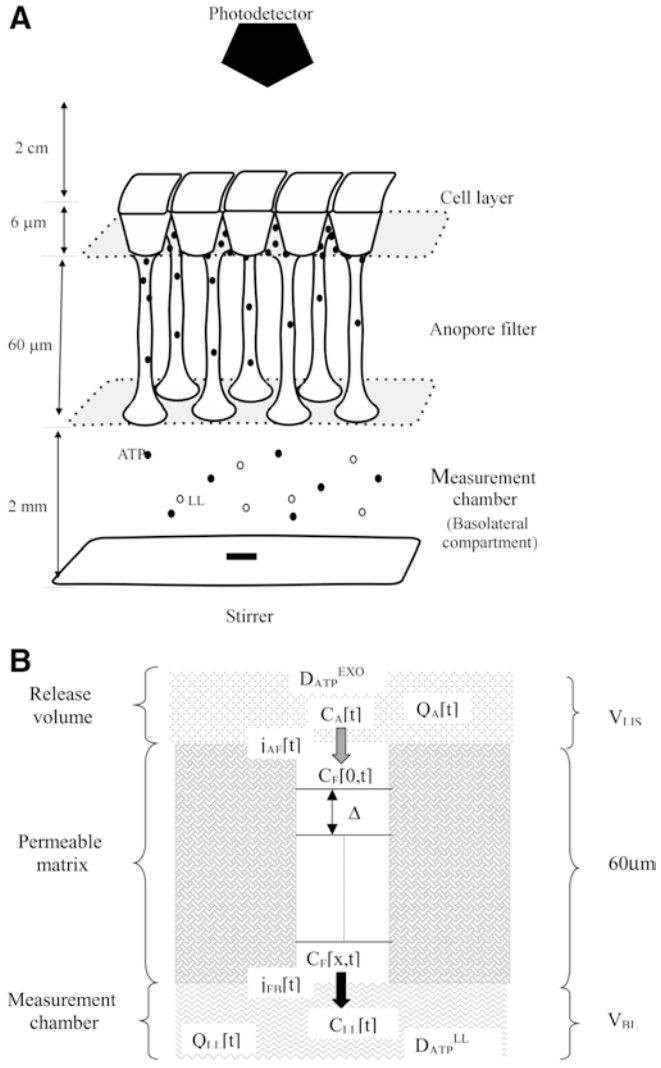

Fig. 1 **A** Experimental set-up: cells are grown in a confluent monolayer on the top of the permeable support mounted in a holder that separates the basolateral and apical compartments of the set-up. The hyposmotic shock imposed by lowering the osmolality of the basolateral bath (the measurement chamber) determines the release of the ATP from the cells into the filter and further into the measurement chamber, where it reacts with the luciferin–luciferase assay kit. The photons emitted are detected by a photon counting tube and the light impulses are further processed using a PC-based 32-bit counter/time board and custom-built software. **B** Modeling layout: the ATP is considered to be released, in response to an osmotic hyposhock, with a constant release rate R_{ATP}, in a small volume V_{LIS} beneath the cell layer; degradation due to exo-enzymes present on the cell membrane is associated with the parameter $D_{ATP}{}^{EXO}$. Inside the filter, ATP diffusion is governed by concentration gradients at the upper and lower sides of the filter, of V_{LIS} and V_{BL} (volume of the measurement chamber), respectively, $\frac{dC_{AF}[t]}{dx} = \frac{C_F[0,t]-C_A[t]}{\Delta x}$ and $\frac{dC_{FB}[t]}{dx} = \frac{C_{LL}[t]-C_F[x=60\ \mu m,t]}{\Delta x}$, and the filter characteristics (pore size and width). J_{AF} and j_{BF} are fluxes through the upper and lower sides of the filter. The stability criterion determines the maximum step over the dimension axis Δx

The well-known one-dimensional diffusion equation along a cartesian axis is essentially an equation for the conservation of mass:

$$\frac{\partial C(x,t)}{\partial t} = D\frac{\partial^2 C(x,t)}{\partial x^2} \tag{2}$$

Analytical solutions are only possible in special cases. Moreover, solutions are highly dependent on the initial and boundary conditions that shape the concentration profile. For this study we have used the Mathematica 4.0 environment (Wolfram Research) and custom-made routines based on a finite differencing scheme through which the set of coupled differential equations, modeling the experimental conditions, was numerically solved.

Using computer simulations we attempted to determine the possible concentration profiles above and below the filter. We derived the complete set of equations associated with ATP release, diffusion towards, into and out from the permeable support, with the measurement via the LL reaction. A diagram of the modeling "layout" is presented in Fig. 1B. Based on experimental conditions, several assumptions have been made:

1. The tightness of the epithelial monolayer ensures that only the ATP released on the basal side of the polarized epithelium is recorded and that ATP does not leak from the apical compartment.
2. The monolayer is able to release (R_{ATP} is the associated release rate) as well as to degrade extracellular ATP through exo-enzymes or ecto-apyrases. The rate of degradation (D_{ATP}^{exo}) depends on the total amount of ATP in the vicinity of the basolateral membrane of the monolayer.
3. ATP diffuses away, through the filter, into the measurement compartment, at a rate of diffusion R_{Diff}, which depends on the ATP concentration near the cell layer, on the concentration gradient inside the filter and on the constant of diffusion inside the permeable support.
4. Instantaneous mixing of the ATP released from the permeable matrix is obtained by the stirring system.
5. The measurement of ATP via LL detection gives rise to consumption of the ATP and inactivation of the LL assay. A global degradation rate, D_{ATP}^{LL}, accounting for the two processes is considered for the measurement chamber.

Based on these assumptions, the following equations are proposed. For the amount of ATP at the cell side of the filter (Q_A):

$$\frac{dQ_A[t]}{dt} = R_{ATP}[t] - D_{ATP}^{exo}Q_A[t] - R_{Diff}[t] \tag{3}$$

The rate of diffusion, R_{Diff}, is proportional to the flux through the filter (in the uppermost layer of the filter) given by:

$$j_{AF}[t] = -D_w\frac{dC_{AF}}{dx} \tag{4}$$

where D_w stands for the diffusion constant of ATP in water [numerous studies suggest that the diffusion of ATP in cytosolic space is only two times lower than in water (de Graaf et al. 2000); in cytoplasm it is 0.15×10^{-5} cm^2 s^{-1}]. dC_{AF}/dx is the concentration gradient between the layer beneath the cells and the upper inside surface of the filter, given by:

$$\frac{dC_{AF}[t]}{dx} = \frac{C_F[0,t] - C_A[t]}{\Delta x} \tag{5}$$

with:

$$C_F[0,t] = \frac{Q_{Diff}[t]}{V_F} \tag{6}$$

where $Q_{Diff}[t]$ is the amount of ATP entering the filter and is related to j_{AF}.

The concentration in the compartment above the filter is:

$$C_A[t] = \frac{Q_A[t]}{V_{LIS}} \tag{7}$$

V_{LIS} is estimated at 1.6×10^{-4} mL; ATP is considered to be released in the lateral interspace that accounts for 5.5% of the cell volume; the thickness of the A6 epithelium is 6.27 µm (Van Driessche et al. 1999).

This process (Eqs. 4, 5, 6, 7) must be equated, due to the porosity of the filter which decreases the active surface and alters the dynamics of the flux. Inside the filter (V_F, the pores total volume, was estimated to 0.01 mL for larger pore filters and 0.015 mL for smaller pore filters), we have considered the transport in one-space dimension, for which the diffusion equation has, according to Fick's second law, the form:

$$\frac{\partial C_F(x,t)}{\partial t} = D_F \frac{\partial^2 C_F(x,t)}{\partial x^2} \tag{8}$$

The presence of physical restricting barriers – the porous support – makes the effective diffusion coefficient, D_F, dependent on the shape, the size and the permeability of the restricting barriers, as well as on the diffusion time.

The dimensions of the pores, 0.2 μm and 0.02 μm, and the uniform tubular shape they retain throughout the filter thickness, imply that this process could be foreseen as free diffusion. Yet, owing to the negative charge of ATP, inside the filter (made out of aluminum oxide with a highly controlled, uniform capillary pore structure) ATP could electrostatically interact with the walls of the pores and be bound inside the filter; therefore the diffusion constant in the filter is considered smaller than the one in water, $D_F < D_W$, and dependent on pore size (for 0.2 μm pore filters, $D_F = 5.5\times10^{-8}$ cm^2 s^{-1}; for 0.02 μm pore filters, $D_F = 3.3\times10^{-8}$ cm^2 s^{-1}). Cell-free experiments (not presented in this article), in which different concentrations of ATP are injected on the apical side of the filter (having no cells attached) and the release rates from the filter are measured, were the basis for the chosen values for the diffusion constant inside the permeable support.

The diffusion flux at the basal side of the filter is related to the concentration gradient between the inside of the filter and the measurement chamber:

$$j_{FB}[t] = -D_F \frac{dC_{FB}}{dx} \tag{9}$$

where dC_{FB}/dx is given by:

$$\frac{dC_{FB}[t]}{dx} = \frac{C_{LL}[t] - C_F[x = 60\ \mu m, t]}{\Delta x} \tag{10}$$

The measurement chamber is well stirred so the concentration in the uppermost layer equals the concentration in the whole measurement chamber. Therefore the concentration in the measurement chamber is expressed as:

$$C_{LL}[t] = \frac{Q_{LL}[t]}{V_{BL}} \tag{11}$$

Taking into account the degradation coefficient D^{LL}_{ATP}, the time evolution of the ATP amount in the measurement chamber is expressed by the following equation:

$$\begin{aligned} \tfrac{dQ_{LL}[t]}{dt} &= R_{release}[t] - D^{LL}_{ATP} Q_{LL}[t-1] \\ \text{where } R_{release}[t] &= \tfrac{dQ_F[t, x=60\ \mu m]}{dt} \end{aligned} \tag{12}$$

$Q_{LL}[t]$ is the amount of ATP in the measurement chamber and D^{LL}_{ATP} is the rate of consumption of ATP due to the LL reaction.

To solve the equations for a membrane–filter–measurement chamber system, we assume a regular distribution for the system variables onto a lattice grid and then solve a finite-difference representation of the equations on the grid. The self-consistent solutions of these equations are obtained using a Forward Time Centered Space algorithm including zero-flux boundary conditions for lattice points next to the cell membrane and filter walls as well as the initial conditions (release rates, breakdown constants). One should note that this algorithm is fully explicit and requires evolving through discrete steps (with the dimension dictated by the stability criterion) towards the spatial scale of interest. Since the time scale of interest is in the order of tens of seconds, this algorithm proved to be reliable and fast, providing the time evolution of the concentration features of every volume unit of the grid. If a broader time scale is required, one could always use the Crank–Nicolson algorithm, which can be easily implemented and provides a good stability for every time step.

The maximum step over the dimension axis was determined, by considering the time step Δt as unity, as $\Delta x = \sqrt{2D}$, in accordance with the stability criterion of the differencing scheme:

$$\frac{2D\Delta t}{(\Delta x)^2} \leqslant 1 \tag{13}$$

The NDSolve routine in Mathematica 4.0 was used for finding solutions to the set of coupled differential equations (Eqs. 3, 4, 5, 6, 7, 8, 9, 10, 11, 12) associated with the system with different permeable supports while changing the ATP generation rates.

Results

To complete the analysis of the ATP release process in response to osmotic shock, the continuous and pulse protocol measurements were complemented with computer simulations of the accumulation profiles near the cell layer and in the measurement chamber. In an accumulation protocol, arresting the perfusion of the LL-containing solution results in a gradual increase in luminescence that shows, after ~20 min, a tendency to reach a plateau. Figure 2A illustrates a typical experiment where ATP accumulation was continuously monitored, during hypotonic conditions, after interruption of the perfusion and addition of LL reagents in the basolateral compartment. A typical recording after successive washouts and additions of LL reagents in the basolateral compartment is shown in the insert. The time course of the total amount of ATP in the measurement chamber obeys Eq. (12), reflecting both the release and consumption rates. Figure 2B presents a typical experiment using the pulse protocol during the hyposmotic shock as well as after the return to isosmotic conditions. Experimental data reveal a biphasic pattern of ATP release in the measurement chamber in response to hyposmotic conditions, consisting of a transient phase of higher release rates followed by a long-term, steady release rate (Fig. 3). A correlation between the ATP accumulation profile and the ATP release from the cell layer can be demonstrated by taking into account the diffusion of ATP through the permeable support.

In order to evaluate the actual dynamics of ATP release from the A6 cell layer, we simulated the time course of the accumulation of ATP near the cell layer and in the measurement chamber, considering several patterns of ATP generation (i.e. constant, pulse and mixed) in a thin layer adjacent to the permeable matrix. Computer simulations (Fig. 4) reveal that the diffusional barrier represented by the permeable support determines a significant delay of the ATP accumulation in the measurement chamber in comparison to the actual dynamics near the cell layer

We used different patterns of ATP release from the cells to simulate the biphasic behavior obtained experimentally (Fig. 3): (1) a single pulse (50 pmol min^{-1} starting 5 s after the onset of hypo conditions

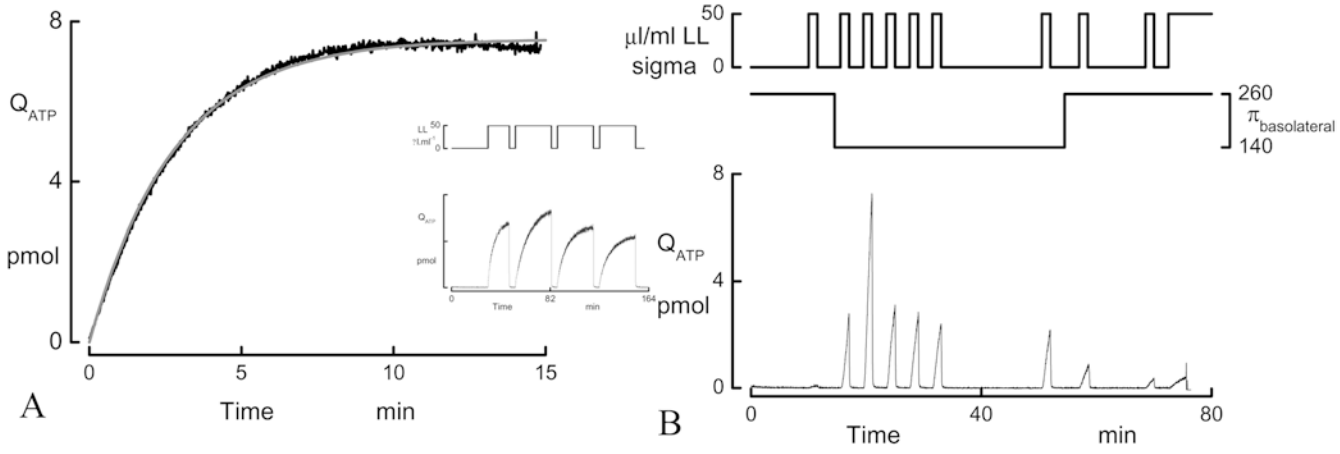

Fig. 2 **A** Continuous ATP accumulation measurement. The hypotonic shock was initiated by reducing the osmolality of the perfusing solution from 260 mosmol $(kg\ H_2O)^{-1}$ to 140 mosmol $(kg\ H_2O)^{-1}$ by removal of NaCl. ATP accumulation is recorded during hypotonicity after addition of the LL reagent and interruption of the perfusion. R_{ATP} and D_{ATP} were determined by fitting an exponential function, $Q_{ATP} = \frac{R_{ATP}}{D_{ATP}}(1 - e^{-D_{ATP}t})$, to the data: $R_{ATP} = 2.72$ pmol min^{-1} and $D_{ATP} = 0.36\ min^{-1}$. **B** Typical pulse protocol recordings. The perfusion was interrupted during 90 intervals after 5 mL of the LL-containing solutions had passed through the basolateral bath. The sensitivity and high dynamic range of the photon counter enables the determination of R_{ATP} in iso- as well as in hyposmotic conditions [260 mosmol $(kg\ H_2O)^{-1}$ and 140 mosmol $(kg\ H_2O)^{-1}$, respectively]. The basolateral osmolality (π) was reduced to 140 mosmol $(kg\ H_2O)^{-1}$ while continuously perfusing at a rate of 5 mL min^{-1}

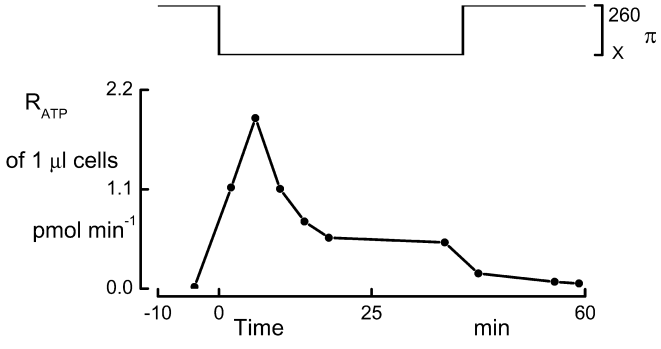

Fig. 3 Time course of R_{ATP} during and after hyposmotic shocks. Probing of ATP release was performed in isosmotic conditions prior to and after the hypotonic shock, and in hyposmotic conditions at 2, 6, 10, 14, 18 and 37 min

and lasting for 15 s); (2) a constant generation rate, $R_{ATP}^{gen} = 3$ pmol min^{-1}; and (3) a mixture of constant and pulse-shaped rates (a 15 s pulse accounting for $R_{ATP}^{gen} = 50$ pmol min^{-1} appearing 4 min after the onset of hyposmotic conditions superimposed on a plateau of $R_{ATP}^{gen} = 3$ pmol min^{-1}). Figure 5A depicts the time course of the amount of ATP near the membrane for the three patterns of ATP generation. Figure 5B shows the accumulation profiles revealed by the pulse protocol for the three shapes of the ATP generation rates. Figure 5C illustrates the simulation of the pulse protocol for the three patterns of ATP generation. The simulations proved that the biphasic behavior obtained experimentally (Figs. 2B, 3) cannot be accounted for by considering only the diffusion dampening and delaying effects as well as constant or pulse R_{ATP} generation rates. Consequently, for both accumulation and pulse protocols, the ATP profiles above and below the permeable matrix when the generation rate is variable in time were computed. The physiological reason behind this approach is based on the documented transient closure of the lateral interspace in A6 cells in response to hyposmotic shock. As will be further elaborated in the Discussion, this transient closure could have a modulating effect on the dynamics of ATP release. The data suggest that the ATP generation profile should contain a mixture of constant and stepwise generation rates to provide an evolution similar to the experimental one; in the following, this pattern was used for the simulations.

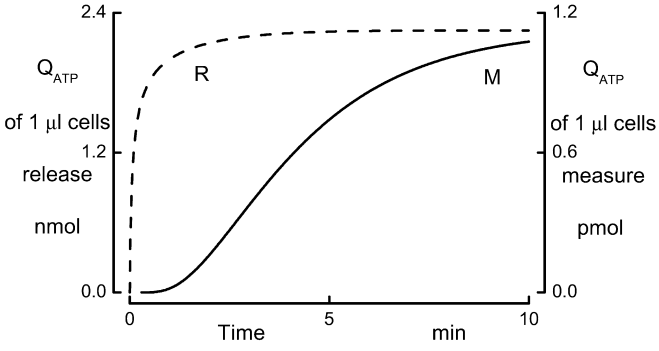

Fig. 4 Simulation of ATP accumulation in the measurement chamber (M) in comparison with the one near the cell layer (R). A marked delay is observed, caused by the diffusion barrier constituted by the permeable support. The value of the diffusion constant in the filter used for the simulation is 5.5×10^{-8} $cm^2\ s^{-1}$. Q_{ATP} release represents the estimated amount of ATP accumulated near the cells for a constant generation rate, $R_{ATP}^{gen} = 3$ pmol min^{-1}, for the whole epithelial surface, a rate of destruction of $D_{ATP}^{exo} = 0.25\ min^{-1}$ and diffusional flow through the filter (curve R). A consumption constant, $D_{ATP}^{exo} = 0.007\ min^{-1}$, caused by the LL oxidative reaction was assumed for the measurement chamber (Q_{ATP} measured represents the time course of the ATP amount in the measurement chamber)

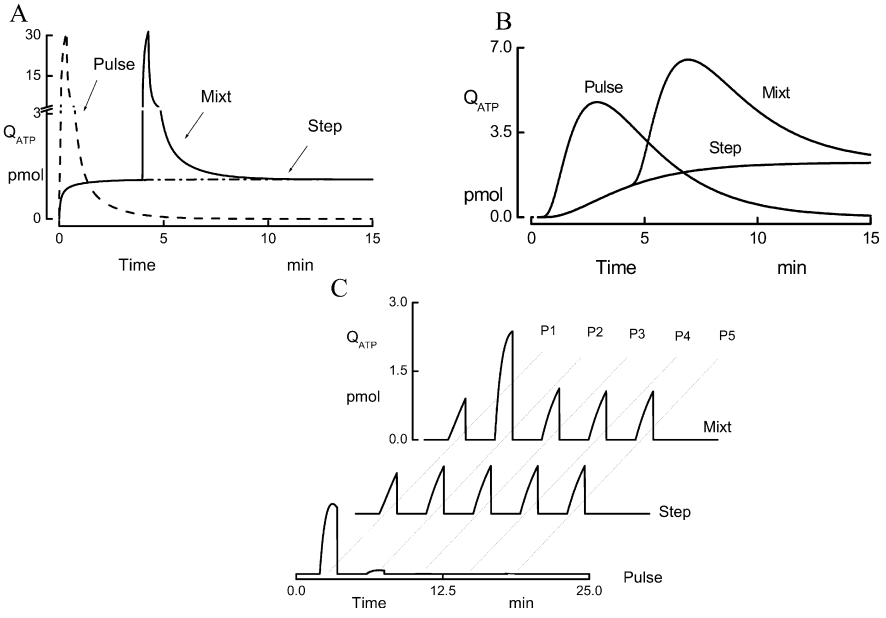

Fig. 5A–C Computer simulations of the time course of the amount of ATP in the measurement chamber when different generation patterns near the cell layer are considered. **A** The simulated evolution of the amount of ATP generated (near the cell monolayer) for: *Pulse*, a single pulse (a 15 s pulse accounting for $R_{ATP}^{gen} = 50$ pmol min^{-1} appearing 5 s after the onset of hypoosmotic conditions); *Step*, constant generation, $R_{ATP}^{gen} = 3$ pmol min^{-1}, for the duration of the hyposmotic shock; and *Mixt*, a mixture of constant and pulse generation rates (a 15 s pulse accounting for $R_{ATP}^{gen} = 50$ pmol min^{-1}, appearing 4 min after the onset of hypoosmotic conditions superposed on a plateau of $R_{ATP}^{gen} = 3$ pmol min^{-1}). **B** The evolution of the accumulated ATP in the measurement chamber for the three release profiles, with indices corresponding to the same conditions as in **A**. **C** The ATP amounts revealed by the pulse protocol for the three release profiles, with indices corresponding to the same conditions as in **A**

It must be stressed that the pulse protocol provides an accurate experimental tool to discern minute changes of the release rates that could, in a continuous protocol, be overlooked.

The global diffusion constant (encompassing possible interaction of the molecules with the permeable matrix) that determines the dynamics of the average movement of ATP molecules towards regions of lower concentration should be dependent to some extent on the structural properties of the available pores. It is conceivable that, if the delay in the measured response is mainly due to the diffusional barrier represented by the filter, the filter characteristics (porosity and pore diameter) would alter the dynamics of the ATP accumulation in the measurement chamber. Therefore we tested the effect of permeable matrices with different pore sizes and porosities: (1) an Anopore filter having larger pores (LP) with 10^9 pores cm^{-2}, 0.2 μm pore diameter and an associated 30% porosity; and (2) smaller pores (SP) with an Anopore filter having 10^{11} pores cm^{-2}, 0.02 μm pore diameter and a 50% associated porosity. We considered a slightly decreased diffusion constant for the SP filter in comparison with the one associated with the LP, in conjunction with possibly enhanced interactions between ATP and the filter.

Computer simulations presented in Fig. 6 suggest that for a SP permeable matrix, assuming a decreased diffusion constant (~60% from the one corresponding to large pores), the dynamics of the ATP accumulation in the measurement chamber, revealed by both continuous measurements and the pulse measurement protocol, will not only be slowed down but there will be a decrease in the measured plateau values as well. Despite the biological variability, the experimental results show a good correlation with the theoretical assumptions: a lower measured rate of ATP release for SP filters. Figure 7 shows, for comparison, the experimental (E) and computed (S) accumulation rates revealed by the pulse protocol. In terms of simulation, the values of the parameters and the rate of degradation, as well as the value of the LIS volume, affect the absolute amounts of ATP in the "measurement chamber" (as well as near the cell layer) and could be adjusted for a closer match with the experimental values. This should be further considered in view of the nonlinear fitting of real data.

Discussion

The present study addresses, from both theoretical and experimental points of view, the problem of ATP release across the basolateral membrane in A6 cells in response to hypotonic treatment and the effect of support permeable matrices in modulating the measured dynamics of ATP accumulation. Computer simulations substantiate the fact that owing to the diffusional barrier represented by the permeable support on which the cells are grown, the dynamics of the ATP accumulation in the measurement chamber is largely delayed in comparison to the concentration change near the cell border. This observation encouraged us to reconsider possible

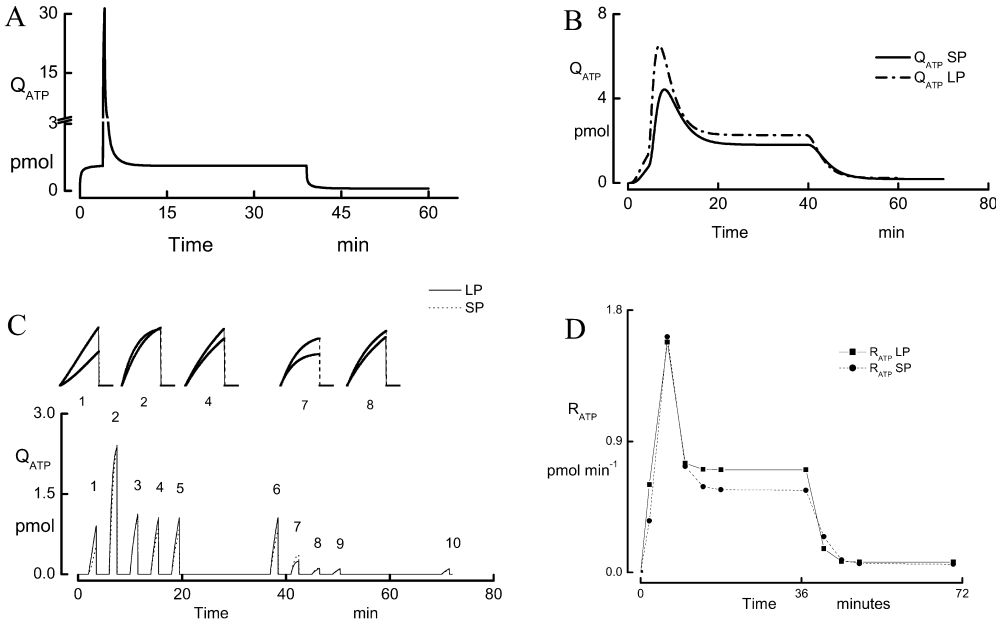

Fig. 6A–D The effect of the diffusion associated with two types of permeable supports: large pores (LP) and small pores (SP), having 0.2 μm and 0.02 μm pore diameters, respectively, on the ATP profiles above and below the permeable support in response to a sequence of hypo- and isosmotic conditions (after returning to ISO a small but constant R_{ATP}^{gen} is considered = 0.3 pmol min^{-1}). **A** Calculated ATP accumulation profile near the cell layer. **B** Evolution of accumulated ATP amount. **C** The same evolution as revealed by pulse measurement protocol. **D** Estimated $R_{ATP}^{release}$ rates from pulse protocols for the simulated data

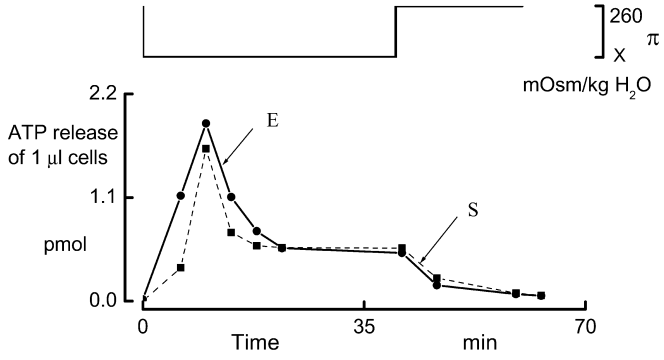

Fig. 7 Comparison between simulated (S) and experimental data (E) related to the ATP accumulation rates revealed by the pulse protocol. A mixture of constant and pulse generation rates (a 15 s pulse accounting for $R_{ATP}^{gen} = 50$ pmol min^{-1} appearing 4 min after the onset of hyposmotic conditions superposed on a plateau of $R_{ATP}^{gen} = 3$ pmol min^{-1}) near the cell layer was considered

correlations between intracellular events (with fast dynamics, e.g. the occurrence of the $[Ca]_i$ peak) and para- and autocrine signaling via ATP. The involvement of extracellular ATP signaling has been demonstrated in response to mechanical (Homolya et al. 2000) and osmotic shocks. Particularly, the ATP release in response to osmotic variations (Hamada et al. 1998; Hazama et al. 1999; Van der Wijk et al. 1999; Kimura et al. 2000; Schwiebert and Kishore 2001; Hisadome et al. 2002) and the related involvement in volume regulation (Wang et al. 1996; Roman et al. 1997; Lange 2000; Knight et al. 2002; Leipziger 2003) have been extensively studied.

Recent studies have revealed a significant involvement of Ca^{2+} signaling in both mechanical and osmotic stress responses (Gordjani et al. 1997; Mahoney et al. 1998; Ostrom et al. 2000; Stout et al. 2002; Woda et al. 2002). Here we focus on the possible correlation between ATP release and intracellular events, most notably the Ca^{2+} mobilization from intracellular stores (Jans et al. 2002). The relation between ATP release and $[Ca^{2+}]_i$ rise has been recently addressed (Jans et al. 2002), but a direct correlation between ATP release and the suramin-sensitive increase in $[Ca^{2+}]_i$ during hypotonicity was shadowed by the time lag between the $[Ca^{2+}]_i$ peak and R_{ATP}^{peak}. The delay of the measured ATP peak can be related to: (1) the unstirred layer effect; (2) closure of the lateral intercellular spaces (LIS), a rapid transient closure of the LIS during cell swelling described previously (Van Driessche et al. 1999); (3) the hindered diffusion of ATP into the bulk fluid (through the permeable support). The improved experimental procedure incorporating a magnetic stirrer (Jans et al. 2002) in the measurement chamber reduced unstirred layers in the chamber. Comparison of the results from computer simulations and experimental data showed that the permeable support indeed introduces a marked delay for ATP diffusion. This result supports the correlation of apparently time-separated events: the occurrence of the $[Ca^{2+}]_i$ peak and the ATP release. However, the simulations showed that diffusion limitation alone cannot mimic the time course of ATP accumulation and ATP release (presented in Figs. 2 and 3). A biphasic feature in ATP generation, involving larger release rates imposed with a significant delay over a "basal" value, has to be introduced to obtain similar patterns for R_{ATP} and Q_{ATP}

as recorded experimentally. To our knowledge, there is no information regarding specific processes that would lead, for the same degree of osmotic insult, to increased ATP release rates. Therefore we analyse our findings in view of the hypothesis that a temporary entrapment of ATP might provide this biphasic behavior, while considering a constant ATP release maintained for the whole duration of the osmotic stress. The documented closure and reopening of the LIS (Van Driessche et al. 1999) during osmotic shock provides the suitable physiological framework for the delayed and augmented ATP release. Previous data from our laboratory (Van Driessche et al. 1999) have shown that the LIS closes rapidly after imposing the hyposmotic challenges and opens with a delay of up to 3 min. Such a mechanism will capture ATP released from the cells in the LIS and release it for diffusion through the filter matrix after opening. Unfortunately, there are extreme experimental difficulties in addressing the issue of ATP compartmentalization in the LIS, but the calculations presented in this study could provide an indirect proof of this matter.

Since the first Ca peak occurs 30 s after the hyposmotic shock and its appearance is blocked by inhibitors of the purinergic receptors (e.g. suramin), it is conceivable that the local [ATP] levels required to activate the purinergic receptors are attained before that moment, via an immediate release of ATP from the basolateral membrane following the hyposhock. Nevertheless, the complete ATP release pattern is far from being resolved; therefore, with the support of the computer simulation presented in this study, we propose a scheme for ATP release that would provide (taking into account the diffusion through the permeable matrix) an evolution consistent with the measured experimental data.

The ATP release is assumed to start a few seconds after the hyposmotic shock and its accumulation, due to the compartmentalization in the LIS [the transient closure is proved by complementary capacitive measurements (Van Driessche et al. 1999)] will reach very soon the physiological levels required to activate the purinergic receptors and to trigger the intracellular Ca peak. Since the surface of the LIS is far larger than the one of the basal membrane, for the same release rate of the ATP considered over the whole basolateral surface of the A6 cell, the closure of the LIS provides ''locally enhanced'' ATP concentrations. At the same time, the ATP released through the basal membrane is diffusing away through the filter. After some delay (due to the diffusional barrier provided by the porous matrix) it reaches the measurement chamber, where it is instantly mixed with the LL assay and is measured. Accordingly, one measures in the first pulse protocol a certain release rate of ATP (Fig. 2B). The release rate is directly connected with the flux of ATP molecules leaving the pores of the filter. According to Fick's law, the flux is proportional to the concentration gradient, and since the pulse protocol involves zero ATP concentration in the measurement chamber at the beginning of the pulse, it is proportional to the concentration on the upper side of the filter.

Under a constant release rate assumption, on the basal side of the cells the ATP is continuously diffusing away, while in the LIS the accumulation of ATP reaches a level that triggers, in conjunction with other intracellular signals, a volume regulatory mechanism (regulatory volume decrease) that determines the re-opening of the LIS and the release of the trapped ATP. Even considering a lower diffusion constant related to the LIS, it would take only seconds until the ATP ''pulse'' (Fig. 4) reaches the upper side of the filter and diffuses away through it. The opening of the LIS is fully accomplished in up to 4 min after the hyposhock (Van Driessche et al. 1999). Considering this time scale, one could understand why the second pulse protocol (Fig. 5) provides a higher release rate of ATP from the filter. It only illustrates the additional amount of ATP present on the upper side of the filter due to the discharge of ATP from the LIS ''store''. We stress once again the fact that what is actually measured is the release rate of ATP from the filter and not the rate of ATP generation from the cell layer.

The ATP generation rate remains constant during the whole interval, and yet, one measures dynamics related to the ''availability'' of the released ATP. After this ''pulse'', the ATP amount on the upper side of the filter equilibrates again to a value related to the constant generation rate, the breakdown constants and the flux into the filter. Correspondingly, one determines a quasi-constant release rate throughout the third and following pulses (the R_{ATP}^{plat}). It is conceivable that the cells keep their ATP generation rate constant as long as the osmotic insult is maintained.

When turning back to the normal isosmotic conditions (ISO), the ATP release rate is either stopped or greatly diminished and the following pulse protocols provide release rates decaying towards near-zero values (Figs. 3 and 6D). Although the local concentration of ATP might have been high, after stopping the ATP generation by returning to ISO, the degradation and the washout of the ATP between the pulses determine its rapid decrease, and accordingly, smaller and smaller release rates from the filter into the measurement chamber. The fact that after subtraction of the background the release rates are not zero, even after long times (i.e. the last pulse is 31 min after the return to ISO conditions), can either account for a small but continuous ATP generation (the ''maintenance'' physiological level) or for a possible washout of the ATP bounded inside the pores of the filter.

Considering the influence of the characteristics of the permeable matrix (pore size and porosity) on the dynamics of the measured ATP, as revealed by both experiment and simulation (Fig. 7), we stress the necessity to use the same kind of permeable support when comparing different sets of experiments. In addition, a possible influence of the support on the characteristics of the epithelium cannot be ruled out. A systematic study (Helman and Liu 1997) showed an effect of the support matrix on the electrical characteristics of confluent monolayers.

The advantage of the experimental method used in this study relies on the fact that it enables continuous, non-invasive estimation of the amount of ATP released basolaterally from a polarized epithelium in response to osmotic shock. In conjunction with appropriate modeling of the diffusion through the permeable support, the method might provide complementary experimental proof of indirectly connected processes like the closure and opening of the LIS.

Acknowledgements This work was supported through the Bilateral Agreement Flanders-Romania (BIL/00/26), the "Fonds voor Wetenschappelijk Onderzoek Vlaanderen" (G.0277.03) and the "Foundation Alphonse en Jean Forton".

References

Bell PD, Lapointe JY, Sabirov R, Hayashi S, Peti-Peterdi J, Manabe K, Kovacs G, Okada Y (2003) Macula densa cell signaling involves ATP release through a maxi anion channel. Proc Natl Acad Sci USA 100:4322–4327

Braunstein GM, Roman RM, Clancy JP, Kudlow BA, Taylor AL, Shylonsky VG, Jovov B, Peter K, Jilling T, Ismailov I, Benos DJ, Schwiebert LM, Fitz JG, Schwiebert EM (2001) Cystic fibrosis transmembrane conductance regulator facilitates ATP release by stimulating a separate ATP release channel for autocrine control of cell volume regulation. J Biol Chem 276:6621–6630

Burnstock G (1997) The past, present and future of purine nucleotides as signalling molecules. Neuropharmacology 36: 1127–1139

de Graaf RA, van Kranenburg A, Nicolay K (2000) In vivo (31)P-NMR diffusion spectroscopy of ATP and phosphocreatine in rat skeletal muscle. Biophys J 78:1657–1664

Gomi K, Kajiyama N (2001) Oxyluciferin, a luminescence product of firefly luciferase, is enzymatically regenerated into luciferin. J Biol Chem 276:36508–36513

Gordjani N, Nitschke R, Greger R, Leipziger J (1997) Capacitative Ca^{2+} entry (CCE) induced by luminal and basolateral ATP in polarised MDCK-C7 cells is restricted to the basolateral membrane. Cell Calcium 22:121–128

Grygorczyk R, Hanrahan JW (1997) CFTR independent ATP release from epithelial cells triggered by mechanical stimuli. Am J Physiol 272:C1058–C1066

Hamada K, Takuwa N, Yokoyama K, Takuwa Y (1998) Stretch activates Jun N-terminal kinase/stress-activated protein kinase in vascular smooth muscle cells through mechanisms involving autocrine ATP stimulation of purinoceptors. J Biol Chem 273:6334–6340

Hazama A, Shimizu T, Ando-Akatsuka Y, Hayashi S, Tanaka S, Maeno E, Okada Y (1999) Swelling-induced, CFTR-independent ATP release from a human epithelial cell line: lack of correlation with volume-sensitive Cl(−) channels. J Gen Physiol 114:525–533

Helman SI, Liu X (1997) Substrate-dependent expression of Na^+ transport and shunt conductance in A6 epithelia. Am J Physiol 273:C434–C441

Hisadome K, Koyama T, Kimura C, Droogmans G, Ito Y, Oike M (2002) Volume-regulated anion channels serve as an auto/paracrine nucleotide release pathway in aortic endothelial cells. J Gen Physiol 119:511–520

Homolya L, Steinberg TH, Boucher RC (2000) Cell to cell communication in response to mechanical stress via bilateral release of ATP and UTP in polarized epithelia. J Cell Biol 150: 1349–1360

Jans D, De Weer P, Srinivas SP, Lariviere E, Simaels J, Van Driessche W (2002) Mg(2+)-sensitive non-capacitative basolateral Ca(2+) entry secondary to cell swelling in the polarized renal A6 epithelium. J Physiol (Lond) 541:91–101

Jans D, Srinivas SP, Waelkens E, Segal A, Lariviere E, Simaels J, Van Driessche W (2002) Hypotonic treatment evokes biphasic ATP release across the basolateral membrane of cultured renal epithelia (A6). J Physiol (Lond) 545:543–555

Kimura C, Koyama T, Oike M, Ito Y (2000) Hypotonic stress-induced NO production in endothelium depends on endogenous ATP. Biochem Biophys Res Commun 274:736–740

Knight GE, Bodin P, De Groat WC, Burnstock G (2002) ATP is released from guinea pig ureter epithelium on distension. Am J Physiol 282:F281–F288

Lange K (2000) Regulation of cell volume via microvillar ion channels. J Cell Physiol 185:21–35

Leipziger J (2003) Control of epithelial transport via luminal P2 receptors. Am J Physiol 284:F419–F432

Mahoney MG, Slakey LL, Benham CD, Gross DJ (1998) Time course of the initial $[Ca^{2+}]_i$ response to extracellular ATP in smooth muscle depends on $[Ca^{2+}]_e$ and ATP concentration. Biophys J 75:2050–2058

Mitchell CH (2001) Release of ATP by a human retinal pigment epithelial cell line: potential for autocrine stimulation through subretinal space. J Physiol (Lond) 534:193–202

Ostrom RS, Gregorian C, Insel PA (2000) Cellular release of and response to ATP as key determinants of the set-point of signal transduction pathways. J Biol Chem 275:11735–11739

Roman RM, Wang Y, Lidofsky SD, Feranchak AP, Lomri N, Scharschmidt BF, Fitz JG (1997) Hepatocellular ATP-binding cassette protein expression enhances ATP release and autocrine regulation of cell volume. J Biol Chem 272: 21970–21976

Roman RM, Lomri N, Braunstein G, Feranchak AP, Simeoni LA, Davison AK, Mechetner E, Schwiebert EM, Fitz JG (2001) Evidence for multidrug resistance-1 P-glycoprotein-dependent regulation of cellular ATP permeability. J Membr Biol 183: 165–173

Romanello M, Pani B, Bicego M, D'Andrea P (2001) Mechanically induced ATP release from human osteoblastic cells. Biochem Biophys Res Commun 289:1275–1281

Schwiebert EM, Kishore BK (2001) Extracellular nucleotide signaling along the renal epithelium. Am J Physiol 280:F945–F963

Stout CE, Costantin JL, Naus CC, Charles AC (2002) Intercellular calcium signaling in astrocytes via ATP release through connexin hemichannels. J Biol Chem 277:10482–10488

Taylor AL, Kudlow BA, Marrs KL, Gruenert DC, Guggino WB, Schwiebert EM (1998) Bioluminescence detection of ATP release mechanisms in epithelia. Am J Physiol 275:C1391–C1406

Van der Wijk T, De Jonge HR, Tilly BC (1999) Osmotic cell swelling-induced ATP release mediates the activation of extracellular signal-regulated protein kinase (Erk)-1/2 but not the activation of osmo-sensitive anion channels. Biochem J 343:579–586

Van Driessche W, De Vos R, Jans D, Simaels J, De Smet P, Raskin G (1999) Transepithelial capacitance decrease reveals closure of lateral interspace in A6 epithelia. Pflugers Arch 437:680–690

Wang Y, Roman R, Lidofsky SD, Fitz JG (1996) Autocrine signaling through ATP release represents a novel mechanism for cell volume regulation. Proc Natl Acad Sci USA 93: 12020–12025

Woda CB, Leite M Jr, Rohatgi R, Satlin LM (2002) Effects of luminal flow and nucleotides on [Ca(2+)](i) in rabbit cortical collecting duct. Am J Physiol 283:F437–F446